

Synthesis, characterization and *in vitro* antitumour activity of diorganotin bisxanthates $[R_2Sn(S_2COR')_2]$ ($R = Me, Et, nBu, Ph$; $R' = Et, iPr, Hex$) and crystal structure of bis(*O*-ethyldithiocarbonato)diphenyltin(IV)*

Neil Donoghue,[†] Edward R. T. Tiekink^{†§} and Lorraine Webster[‡]

[†] Jordan Laboratories, Department of Physical and Inorganic Chemistry, University of Adelaide, GPO Box 498, Adelaide, South Australia 5001, Australia, and [‡] Experimental Chemotherapy and Pharmacology Unit, Peter MacCallum Cancer Institute, 481 Little Lonsdale Street, Melbourne, Victoria 3000, Australia

A series of diorganotin bisxanthate compounds, $[R_2Sn(S_2COR')_2]$ ($R = Me, Et, nBu, tBu$, and Ph ; $R' = Et, iPr$ and $cHex$) have been prepared and characterized by spectroscopic methods (IR, NMR and FAB MS). The xanthate ligands chelate the R_2Sn moieties forming disparate Sn–S bonds leading to skew-trapezoidal biipyramidal tin atom geometries. The crystal structure of a representative compound, $[Ph_2Sn(S_2COEt)_2]$, confirms the spectroscopic results and shows the tin atom to be coordinated by two asymmetrically chelating xanthate ligands [Sn–S(1) 2.486(1), Sn–S(2) 3.052(1) Å and Sn–S(3) 2.484(1), Sn–S(4) 3.220(1) Å] with the two phenyl substituents lying over the weaker Sn–S interactions so that C–Sn–C is 126.5(1)°. Crystal data for $[Ph_2Sn(S_2COEt)_2]$: monoclinic space group $P2_1/n$: $a = 9.645(1)$, $b = 23.723(3)$, $c = 9.798(2)$ Å, $\beta = 100.23(1)^\circ$, $V = 2206.2$ Å³, $Z = 4$; 2708 data refined to final R 0.023. A selection of these compounds has been evaluated for activity against the L1210 mouse leukaemia cell line.

Keywords: Diorganotin, xanthates X-ray, anti-tumour

INTRODUCTION

The use of organotin compounds in a variety of industrial and agricultural applications is well documented.^{1–4} A more recent development is the

exploration of the anti-tumour activity of organotin compounds owing to the success of other metal-based species in the search for effective anti-cancer drugs.^{5,6} A wide variety of organotin compounds have been investigated in this context. However, organotin thiolates have not received as much attention as have organotin compounds with oxygen or nitrogen donor ligands. Among the organotin thiolates that have been examined for possible anti-tumour activity are those with various dithiophosphinates⁷ and anions derived from sulphur-containing amino acids,⁸ 6-mercaptopurine⁸ and 3-thiopropionic acid.⁹ This report extends this series of thiolates to include a selection of organotin xanthate ($\sim S_2COR'$) complexes.

Several organotin xanthate complexes are known in the literature and some examples have been characterized by X-ray crystallographic methods.^{10–14} Less well known is the biological activity of metal/xanthate complexes which seems to be restricted only to the phosphinegold(I) xanthates which have been investigated for both their anti-tumour¹⁵ and anti-arthritis activity.¹⁶ This paper reports the preparation of a series of diorganotin bisxanthate compounds, $[R_2Sn(S_2COR')_2]$ ($R = Me, Et, nBu, tBu, Ph$; $R' = Et, iPr$ and $cHex$), their characterization and a preliminary evaluation of their *in vitro* anti-tumour activity.

EXPERIMENTAL

Synthesis

The $[R_2SnCl_2]$ starting materials were purchased from Strem ($R = Me$) and Aldrich Chemical Co. ($R = nBu, tBu, Ph$). $[Et_2SnCl_2]$ was prepared by

* Supplementary material is lodged with the Cambridge Crystallographic Data Centre, UK.

§ Author for correspondence.

Table 1 Analytical and physical data for $[R_2Sn(S_2COR')_2]$

Compound	Physical state	Yield (%)	M.p. (°C)	Analysis (%)			
				C		H	
				Calcd	Obs.	Calcd	Obs.
$Me_2Sn(S_2COEt)_2$	Colourless cryst.	81	95–96	24.57	24.56	4.12	4.06
$Me_2Sn(S_2COiPr)_2$	Colourless cryst.	75	41–42	28.65	28.70	4.81	4.71
$Me_2Sn(S_2COcHex)_2$	Colourless cryst.	72	117–118	38.49	38.51	5.65	5.56
$Et_2Sn(S_2COEt)_2$	Colourless cryst.	68	52–53	28.65	28.73	4.81	5.03
$Et_2Sn(S_2COiPr)_2$	Yellow oil	61	—	32.22	32.16	5.41	5.70
$Et_2Sn(S_2COcHex)_2$	Colourless cryst.	76	81–82	40.99	40.84	6.12	6.39
$nBu_2Sn(S_2COEt)_2$	Pale yellow oil	99	—	— ^a	—	—	—
$nBu_2Sn(S_2COiPr)_2$	Pale yellow oil	87	—	38.18	38.34	6.41	6.89
$nBu_2Sn(S_2COcHex)_2$	Colourless cryst.	93	66–67	45.28	45.43	6.91	6.86
$Ph_2Sn(S_2COEt)_2$	Colourless cryst.	98	88–89	41.95	42.11	3.91	4.03
$Ph_2Sn(S_2COiPr)_2$	Colourless cryst.	41	93–94	44.21	44.23	4.45	4.37
$Ph_2Sn(S_2COcHex)_2$	Colourless cryst.	57	129–130	50.09	49.44	5.17	5.04

^a Reproducible analysis was not obtained for this compound.

the coproportionation of $[SnCl_4]$ (Strem) and $[Et_3SnCl]$ (Strem). The potassium salts of the xanthate ligands were prepared from the appropriate alcohol, potassium hydroxide and carbon disulphide with excess alcohol acting as the solvent. All solvents used were of analytical grade.

All $[R_2Sn(S_2COR')_2]$ complexes were prepared employing a similar procedure to that given for the $[Me_2Sn(S_2COEt)_2]$ compound. To $[Me_2SnCl_2]$ (1.00 g, 4.55 mmol) in dichloromethane (CH_2Cl_2) (50 cm³) was added an ethanolic solution (50 cm³) of $K[S_2COEt]$ (2.19 g, 13.7 mmol) and ammonium chloride (ca. 0.2 g). The mixture was stirred for 0.5 h, filtered and evaporated to dryness. The complex was extracted with a CH_2Cl_2 /ethanol (1:5) solution which, when allowed to stand at 277 K, deposited colourless crystals. Other complexes were prepared similarly and details are listed in Table 1; the $R = tBu$ compounds were characterized by spectroscopic methods only.

Crystallography

Intensity data for colourless crystal (0.38 mm × 0.38 mm × 0.40 mm) of $[Ph_2Sn(S_2COEt)_2]$ were measured at 293 K on an Enraf–Nonius CAD4F diffractometer fitted with graphite-monochromatized $MoK\alpha$ radiation, $\lambda = 0.7107 \text{ \AA}$. The $\omega:2\theta$ scan technique was employed to measure 4580 data up to a maximum Bragg angle of 25.0° . The data set was corrected for Lorentz and polarization effects and for absorption using an analytical procedure; maxi-

mum and minimum transmission factors were 0.641 and 0.591, respectively.¹⁷ There were 3899 unique reflections of which 2708 satisfied the $I \geq 2.5 \sigma(I)$ criterion and were used in the subsequent analysis.

Crystal data for $[Ph_2Sn(S_2COEt)_2]$: monoclinic, space group $P2_1/n$, $a = 9.645(1)$, $b = 23.723(3)$, $c = 9.798(2) \text{ \AA}$, $\beta = 100.23(1)^\circ$, $V = 2206.2 \text{ \AA}^3$, $Z = 4$, $D_c = 1.551 \text{ g cm}^{-3}$, $F(000) = 1032$, $\mu = 14.20 \text{ cm}^{-1}$.

The structure was solved from the interpretation of the Patterson synthesis and refined by a full-matrix least-squares procedure based on F .¹⁷ Non-hydrogen atoms were refined with anisotropic thermal parameters and hydrogen atoms were included in the model at their calculated positions with a common isotropic thermal parameter. After the inclusion of a weighting scheme of the form $w = k[\sigma^2(F) + |g|F^2]$, the refinement was continued until convergence; $R = 0.023$, $k = 0.828$, $g = 0.0006$, $R_w = 0.027$. The analysis of variance showed no special features, indicating that an appropriate weighting scheme had been applied. The maximum residual electron density peak in the final difference map was 0.41 e \AA^{-3} . Fractional atomic coordinates are listed in Table 2 and the numbering scheme employed is shown in Fig. 1 which was drawn with ORTEP¹⁸ at 25% probability ellipsoids. Scattering factors were as incorporated in the SHELX76 program¹⁷ and the refinement was performed on a SUN4/280 computer. Other crystallographic details, com-

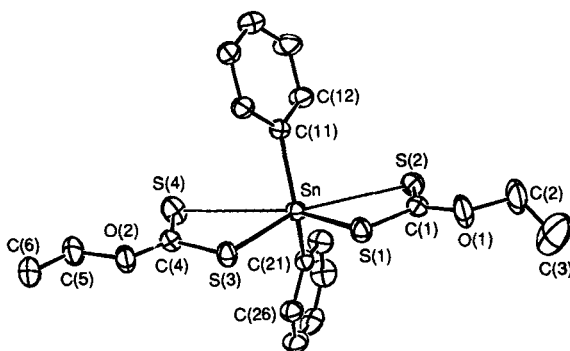
Table 2 Fractional atomic coordinates ($\times 10^5$ for Sn, $\times 10^4$ other atoms) for $[\text{Ph}_2\text{Sn}(\text{S}_2\text{COEt}')_2]$

Atom	x	y	z
Sn	0.20029(2)	0.12596(1)	0.01482(2)
S(1)	0.0777(1)	0.0527(1)	0.1303(1)
S(2)	0.3252(1)	0.1018(1)	0.3177(1)
S(3)	0.0287(1)	0.0987(1)	-0.1949(1)
S(4)	0.1937(1)	0.1979(1)	-0.2649(1)
O(1)	0.1502(4)	0.0234(1)	0.3784(3)
O(2)	-0.0144(3)	0.1466(1)	-0.4275(3)
C(1)	0.1893(4)	0.0591(2)	0.2888(4)
C(2)	0.2373(9)	0.0181(3)	0.5173(5)
C(3)	0.2612(10)	-0.0332(3)	0.5538(9)
C(4)	0.0699(4)	0.1508(2)	-0.3062(4)
C(5)	-0.0003(6)	0.1866(2)	-0.5375(5)
C(6)	-0.1114(6)	0.1744(2)	-0.6555(5)
C(11)	0.1430(3)	0.2071(1)	0.0774(3)
C(12)	0.2335(4)	0.2399(2)	0.1714(5)
C(13)	0.1919(5)	0.2933(2)	0.2035(5)
C(14)	0.0616(5)	0.3142(2)	0.1426(5)
C(15)	-0.0258(5)	0.2825(2)	0.0511(5)
C(16)	0.0142(4)	0.2285(2)	0.0176(4)
C(21)	0.4016(3)	0.1011(2)	-0.0227(3)
C(22)	0.5237(4)	0.1270(2)	0.0427(5)
C(23)	0.6531(5)	0.1114(2)	0.0127(6)
C(24)	0.6611(5)	0.0693(2)	-0.0800(6)
C(25)	0.5423(5)	0.0437(2)	-0.1467(5)
C(26)	0.4113(4)	0.0597(2)	-0.1176(4)

prising thermal parameters, H-atom parameters, all bond distances and angles, and tables of observed and calculated structure factors are available on request from the correspondence author or CCDC.

Biological testing

L1210 mouse leukaemia cells were grown as suspension cultures in MEM (Eagle's Minimum Essential Medium) plus 1% glutamine and 15%

**Figure 1** Molecular structure and crystallographic numbering scheme employed for $[\text{Ph}_2\text{Sn}(\text{S}_2\text{COEt})_2]$.

fetal calf serum (Flow Laboratories). The compounds were dissolved in DMSO at 10 concentrations over a 3-log range, with a final maximum DMSO concentration in the medium of 0.5%. Growth inhibition was tested by incubation log-phase cells at 37 °C in a humidified incubator gassed with 10% CO_2 /90% air for 48 h in the presence of the compound. Cells were then counted using a Coulter counter, and the ID_{50} , in $\mu\text{mol dm}^{-3}$, or dose causing 50% inhibition of cell growth, was determined from the curve of percentage growth versus dose. Control cultures exposed only to the vehicle were included with each test.

Instrumentation

Infrared spectra were measured on a Perkin-Elmer 1720X FT spectrometer as KBr discs or between NaCl plates. NMR spectra were recorded in CDCl_3 solutions on an ACP300 (^1H NMR at 300.13 MHz and ^{13}C NMR at 75.47 MHz) spectrometer; the internal reference was SiMe_4 in both cases. FAB mass spectra were obtained on VG ZAB 2HF instrument equipped with a FAB source. Argon was used as the exciting gas with the source pressure typically 10^{-6} mbar, the FAB voltage was 7 kV and the current 1 mA. The ion-accelerating potential was 8 kV and the matrix employed was 3-nitrobenzyl alcohol. The complexes were made up as *ca* 0.5 mol dm^{-3} solutions in dichloromethane; a drop was added to a drop of the matrix and the mixture was applied to the FAB probe tip.

RESULTS AND DISCUSSION

A series of $[\text{R}_2\text{Sn}(\text{S}_2\text{COR}')_2]$ ($\text{R} = \text{Me}, \text{Et}, \text{nBu}, \text{tBu}, \text{Ph}$; $\text{R}' = \text{Et}, \text{iPr}$ and cHex) compounds have been prepared via the metathetical reaction between R_2SnCl_2 and $\text{K}[\text{S}_2\text{COR}']$. The $\text{R}' = \text{tBu}$ compounds were found to be relatively unstable; thus their characterization is restricted to spectroscopic methods only. The remaining compounds are stable solids or oils; physical data, yields and microanalytical results for these compounds are listed in Table 1.

Infrared data for the $[\text{R}_2\text{Sn}(\text{S}_2\text{COR}')_2]$ compounds are summarized in Table 3. Strong absorptions which are characteristic of xanthate ligands are found in the regions 1270–1181 and 1094–996 cm^{-1} and these are assigned to $\nu(\text{C}-\text{O})$

Table 3 Selected infrared data (cm^{-1}) for $[\text{R}_2\text{Sn}(\text{S}_2\text{COR}')_2]^a$

Compound	$\nu(\text{C}-\text{O})$	$\nu(\text{C}-\text{S})$	$\nu(\text{C}-\text{Sn}-\text{C})$	$\nu(\text{Sn}-\text{S})$
$\text{Me}_2\text{Sn}(\text{S}_2\text{COEt})_2^b$	1234s, 1212s 1195s	1050s, 1031s 1005s	668w, 550m	440m
$\text{Me}_2\text{Sn}(\text{S}_2\text{COiPr})_2^b$	1225s	1087s, 1027s	666w, 558w	454m, 396m
$\text{Me}_2\text{Sn}(\text{S}_2\text{COCocHex})_2^b$	1266s, 1251s 1218s, 1191s	1062s, 1040s 1027s, 999s	668w, 560w	479m, 468m
$\text{Et}_2\text{Sn}(\text{S}_2\text{COEt})_2^b$	1207s	1046s, 1035s 1005s	686m, 527w	439m, 404w
$\text{Et}_2\text{Sn}(\text{S}_2\text{COiPr})_2^c$	1220s	1089s, 1030s	687m	n.o. ^d
$\text{Et}_2\text{Sn}(\text{S}_2\text{COCocHex})_2^b$	1249s, 1211s	1051s, 1012s	687m, 524w	480w, 440w
$\text{nBu}_2\text{Sn}(\text{S}_2\text{COEt})_2^c$	1208s	1040s	683w	n.o. ^d
$\text{nBu}_2\text{Sn}(\text{S}_2\text{COiPr})_2^c$	1224s	1090s, 1031s	684w, 667w	n.o. ^d
$\text{nBu}_2\text{Sn}(\text{S}_2\text{COCocHex})_2^b$	1248s, 1211s 1189s	1056s, 1042s 1026s, 1019s 998s	683w, 668w	477w, 464w
$\text{tBu}_2\text{Sn}(\text{S}_2\text{COEt})_2^b$	1244s, 1188s	1039s, 1005s	940w, 798w	449w, 438w
$\text{tBu}_2\text{Sn}(\text{S}_2\text{COiPr})_2^b$	1238s, 1209s 1181s	1084s, 1030s	939w, 799w	456m
$\text{tBu}_2\text{Sn}(\text{S}_2\text{COCocHex})_2^c$	1252, 1230s 1202s	1044s, 1030s 1020s, 1001s	917m, 892m	n.o. ^d
$\text{Ph}_2\text{Sn}(\text{S}_2\text{COEt})_2^b$	1216s	1040s, 996s	—	446s
$\text{Ph}_2\text{Sn}(\text{S}_2\text{COiPr})_2^b$	1220s, 1190s	1094s, 1083s 1022s, 997s	—	456s, 444s
$\text{Ph}_2\text{Sn}(\text{S}_2\text{COCocHex})_2^b$	1212s	1056, 1040s 1019s, 996s	—	450s

^a s, m and w have their usual meanings. ^b Measured as KBr disc. ^c Measured between NaCl plates. ^d n.o., not observed.

and $\nu(\text{C}-\text{S})$, respectively.¹⁹ In addition, weak-to-medium bands in the region $480\text{--}396\text{ cm}^{-1}$ are assigned to $\nu(\text{Sn}-\text{S})$ for the solid compounds. For the dialkyltin compounds, bands due to $\nu(\text{C}-\text{Sn}-\text{C})$ are observed in the expected regions according to the alkyl group.

The ^1H NMR data are summarized in Table 4 and are consistent with the integration and multiplicities expected for the $[\text{R}_2\text{Sn}(\text{S}_2\text{COR}')_2]$ compounds. The alkyl protons resonated in the usual range of $\delta 0.5\text{--}2.5$ ppm except for the protons bound to $\text{C}(\alpha)$, the C atom bound to the O atom of the xanthate ligand. The phenyl protons resonate at $\delta 7\text{--}8$ ppm. The interesting feature of the spectra was tin-proton coupling, typically about $60\text{--}80$ Hz for α protons and $70\text{--}150$ Hz for β protons on the organic substituents bound to the tin atom. There is a significant downfield shift of the *ortho* protons on the tin-bound phenyl groups which also exhibited coupling to the tin atom.

The ^{13}C NMR data are summarized in Table 5. The carbon atoms resonate at the expected positions and tin-carbon coupling is observed. For a given xanthate ligand, the chemical shifts of S_2COC were characteristic of the ligand (i.e. δ

$71.8\text{--}72.4$ ppm for $\text{S}_2\text{COCH}_2\text{CH}_3$) and did not vary significantly as the nature of the R_2Sn moiety was changed. The chemical shifts for S_2CO in Ph_2Sn compounds were consistently upfield by approximately 3 ppm compared with the remaining R_2Sn complexes, which had values in the narrow range $219.7\text{--}223.1$ ppm. The similarity in the resonances associated with the xanthate ligands suggests a similar coordination mode for these ligands in the complexes. The chemical shifts for S_2CO were systematically downfield for the ethyl xanthate ligand compared with the isopropyl and cyclohexyl xanthate ligands, although it is emphasized that the differences in δ are very small.

Coupling between tin and carbon was observed only for the tin-bound R groups; no coupling was observed involving the xanthate carbon atoms. The coupling constants fall into three groups with $^1J(^{119}\text{Sn}\text{--}^{13}\text{C}(\alpha))$ in the range $419\text{--}437$ Hz for the tBu_2Sn compounds, $525\text{--}595$ Hz for the Ph_2Sn , Et_2Sn and Me_2Sn compounds (with the Ph_2Sn generally having the lower values and the Me_2Sn compounds the higher), and $630\text{--}770$ Hz for the nBu_2Sn compounds. There was no systematic

Table 4 ^1H NMR data (δ , ppm) for $[\text{R}_2\text{Sn}(\text{S}_2\text{COR}')_2]_2^{\text{a}}$

Compound	H(α)	H(β)	H(γ)	H(δ)	H(1)	H(2)	H(3)	H(4)
$\text{Me}_2\text{Sn}(\text{S}_2\text{COEt})_2$	1.46s (79.2) ^b				4.51q (7.12) ^c	1.44t		
$\text{Me}_2\text{Sn}(\text{S}_2\text{COiPr})_2$	1.46s (79.0) ^b				5.43m (6.30) ^c	1.40d		
$\text{Me}_2\text{Sn}(\text{S}_2\text{COCocHex})_2$	1.46s (75.9) ^b				5.20m (4.0) ^c		2.1–1.5 ^d	
$\text{Et}_2\text{Sn}(\text{S}_2\text{COEt})_2$	2.06q (7.78) ^c (63.9) ^b	1.54t (148) ^b			4.53q (7.11) ^c	1.44t		
$\text{Et}_2\text{Sn}(\text{S}_2\text{COiPr})_2$	2.06q (7.78) ^c (63.7) ^b	1.54t (152) ^b			5.44m (6.22) ^c	1.41d		
$\text{Et}_2\text{Sn}(\text{S}_2\text{COCocHex})_2$	2.06q (7.77) ^c (65.5) ^b	1.54t			5.21m (4.38) ^c		2.2–0.8 ^d	
$\text{nBu}_2\text{Sn}(\text{S}_2\text{COEt})_2$	2.1–1.1 ^d (7.25) ^c			0.94t	4.53q (7.08) ^c	1.47t		
$\text{nBu}_2\text{Sn}(\text{S}_2\text{COiPr})_2$	2.2–1.1 ^d (7.38) ^c			0.93t	5.44m (6.23) ^c	1.41d		
$\text{nBu}_2\text{Sn}(\text{S}_2\text{COCocHex})_2$	2.2–1.1 ^d (7.33) ^c (125) ^b			0.93t	5.21m (4.57) ^c		2.2–1.1 ^d	
$\text{tBu}_2\text{Sn}(\text{S}_2\text{COEt})_2$		1.50s (111) ^b			4.47q (7.21) ^c	1.42t		
$\text{tBu}_2\text{Sn}(\text{S}_2\text{COiPr})_2$		1.56 (114) ^b			5.43m (6.14) ^c	1.42d		
$\text{tBu}_2\text{Sn}(\text{S}_2\text{COCocHex})_2$		1.51s —			5.14m (3.96) ^c		2.1–0.8 ^d	
$\text{Ph}_2\text{Sn}(\text{S}_2\text{COEt})_2$		7.95m (86.6) ^b	7.44m ^c		4.29q (7.13) ^c	1.19t		
$\text{Ph}_2\text{Sn}(\text{S}_2\text{COiPr})_2$		7.97 (77.1) ^b	7.44m ^c		5.23m (6.20) ^c	1.11d		
$\text{Ph}_2\text{Sn}(\text{S}_2\text{COCocHex})_2$		7.99m (84.5) ^b	7.47m ^c		4.99m (4.36) ^c		2.1–1.0 ^d	

^a Spectra recorded in CDCl_3 solution except for the tBu compounds which were recorded in CCl_4 solution; H atoms with Greek letters are from the tin-bound R group. ^b $J(^{119}\text{Sn}-^1\text{H})$. ^c $J(^1\text{H}-^1\text{H})$. ^d Overlapping multiplets. ^e Overlapping multiplets due to H γ and H δ .

variation in the values of these coupling constants and the xanthate ligand.

The $[\text{R}_2\text{Sn}(\text{S}_2\text{COR}')_2]$ compounds were subjected to a Fast Atom Bombardment–Mass Spectroscopic (FAB MS) study and the results obtained are listed in Table 6. The most abundant fragment observed in the spectra corresponded to the monoxanthate ion $[\text{R}_2\text{Sn}(\text{S}_2\text{COR}')_2]^+$ although for the Me_2Sn compounds and for the $\text{R}=\text{Ph}$, $\text{R}'=\text{cHex}$ compound this ion was not observed. The most abundant ion for the $[\text{Me}_2\text{Sn}(\text{S}_2\text{COEt})_2]$ compound was the molecular ion $[\text{R}_2\text{Sn}(\text{S}_2\text{COR}')_2]^+$, which was absent or in very low relative abundance in most spectra. For the $[\text{Me}_2\text{Sn}(\text{S}_2\text{COiPr})_2]$ and $[\text{Me}_2\text{Sn}(\text{S}_2\text{COCocHex})_2]$

compounds the $[\text{R}_4\text{Sn}_2(\text{S}_2\text{COiPr})_3]^+$ and $[\text{MeSn}(\text{S}_2\text{COCocHex})(\text{S}_2\text{CO})]^+$ ions, respectively, were the most abundant and these were in the main absent from the spectra of the other compounds. The $[\text{Ph}_2\text{Sn}(\text{S}_2\text{CO})]^+$ fragment was the most abundant for the $[\text{Ph}_2\text{Sn}(\text{S}_2\text{COCocHex})_2]$ compound. Clearly the behaviour of the $[\text{Me}_2\text{Sn}(\text{S}_2\text{COR}')_2]$ compounds contrasts with that of the other R_2Sn derivatives. Except for the ions already mentioned, the spectra were quite featureless with relative low abundances for the remaining species; the highest-nuclearity fragments had a maximum of two tin atoms. A common fragment in all spectra was $[\text{RSn}(\text{S}_2\text{COR}')_2]^+$ in which one of the Sn–R

Table 5 ^{13}C NMR data (δ , ppm) for $[\text{R}_2\text{Sn}(\text{S}_2\text{COR}')_2]^a$

Compound	C(α)	C(β)	C(γ)	C(δ)	S ₂ CO	C(1)	C(2)	C(3)	C(4)
$\text{Me}_2\text{Sn}(\text{S}_2\text{COEt})_2$	10.3 (568) ^b				221.6	72.1	13.8		
$\text{Me}_2\text{Sn}(\text{S}_2\text{COiPr})_2$	10.3 (595) ^b				220.6	80.5	21.2		
$\text{Me}_2\text{Sn}(\text{S}_2\text{COCocHex})_2$	10.4 (581) ^b				220.6	85.3	30.8	23.6	25.0
$\text{Et}_2\text{Sn}(\text{S}_2\text{COEt})_2$	23.7 (564.1) ^b	11.0 (45.8) ^b			223.1	72.0	13.7		
$\text{Et}_2\text{Sn}(\text{S}_2\text{COiPr})_2$	23.6 (541) ^b	10.9 (45.3) ^b			222.1	80.2	21.1		
$\text{Et}_2\text{Sn}(\text{S}_2\text{COCocHex})_2$	23.6 (560) ^b	10.6			221.9	85.0	30.5	23.2	24.7
$\text{nBu}_2\text{Sn}(\text{S}_2\text{COEt})_2$	28.8 (760) ^b	26.2	30.0	13.6	222.6	71.8	13.4		
$\text{nBu}_2\text{Sn}(\text{S}_2\text{COiPr})_2$	28.6 (630) ^b	26.2	30.2	13.5	221.9	80.2	21.2		
$\text{nBu}_2\text{Sn}(\text{S}_2\text{COCocHex})_2$	28.6 (770) ^b	26.1	30.2	13.5	221.7	84.9	30.7	23.5	25.0
$\text{tBu}_2\text{Sn}(\text{S}_2\text{COEt})_2^c$	46.7 (419) ^b	32.0			222.0	71.9	14.6		
$\text{tBu}_2\text{Sn}(\text{S}_2\text{COiPr})_2^c$	46.7 (434) ^b	32.0			219.7	80.2	22.0		
$\text{tBu}_2\text{Sn}(\text{S}_2\text{COCocHex})_2^c$	46.7 (437) ^b	31.9			219.7	85.2	31.6	24.4	25.9
$\text{Ph}_2\text{Sn}(\text{S}_2\text{COEt})_2$	141.3 (525) ^b	135.2 (56.7) ^b	129.0 (86.5) ^b	130.0 (18.5) ^b	218.3	72.4	13.5		
$\text{Ph}_2\text{Sn}(\text{S}_2\text{COiPr})_2$	141.4	135.4 (56.5) ^b	128.9 (82.8) ^b	130.0 (17.4) ^b	217.2	81.1	20.7		
$\text{Ph}_2\text{Sn}(\text{S}_2\text{COCocHex})_2$	141.2 (536) ^b	135.1 (56.9) ^b	128.6 (87.1) ^b	129.7 (17.4) ^b	217.3	86.1	30.3	23.4	24.7

^a Spectra recorded in CDCl_3 solution; C atoms with Greek letters are from the tin-bound R group.^b $J(^{119}\text{Sn}-^{13}\text{C})$. ^c Spectra recorded in CCl_4 solution.

bonds had been cleaved; however, it is worth emphasizing that no one fragment appeared in all spectra.

A crystal structure determination of a representative compound, $[\text{Ph}_2\text{Sn}(\text{S}_2\text{COEt})_2]$, has been carried out and shown to be similar to the previously determined structures of $[\text{Me}_2\text{Sn}(\text{S}_2\text{COEt})_2]$ ¹⁰ and $[\text{Ph}_2\text{Sn}(\text{S}_2\text{COiPr})_2]$.¹¹ The molecule is illustrated in Fig. 1 and selected interatomic parameters are listed in Table 7; there are no significant intermolecular contacts in the lattice. The tin atom is coordinated by two asymmetrically chelating xanthate ligands forming short $[\text{Sn}-\text{S}(1) 2.486(1), \text{Sn}-\text{S}(3) 2.484(1) \text{ \AA}, \text{S}(1)-\text{Sn}-\text{S}(3) 83.9(1)^\circ]$ and long $\text{Sn}-\text{S} [\text{Sn}-\text{S}(2) 3.052(1), \text{Sn}-\text{S}(4) 3.220(1) \text{ \AA}, \text{S}(2)-\text{Sn}-\text{S}(4) 150.7(1)^\circ]$ bond distances. The two tin-bound phenyl groups are disposed so as to lie over the weaker $\text{Sn}-\text{S}$ bonds and subtend an angle of

$126.5(1)^\circ$ at the tin atom. The coordination geometry about the tin atom is best described as being based on a distorted skew-trapezoidal bipyramidal geometry with the four sulphur atoms defining the basal plane. The asymmetry in the mode of coordination of the xanthate ligands is reflected in the associated C-S bond distances. The long C-S bond distances $[\text{C}-\text{S}(1) 1.732(4)$ and $\text{C}-\text{S}(3) 1.742(4) \text{ \AA}]$ involve the sulphur atoms forming the stronger $\text{Sn}-\text{S}$ interactions and the short C-S bond distances $[\text{C}-\text{S}(2) 1.641(4)$ and $1.633(4) \text{ \AA}]$ are associated with the weakly coordinating sulphur atoms.

The C-Sn-C angle of $126.5(1)^\circ$ found in the crystal structure may be compared with 108° , being the angle calculated using the value of the $^1J(^{119}\text{Sn}-^{13}\text{C})$ coupling constant and the empirical relationship between C-Sn-C angles and coupling constants in diphenyltin systems as reported

Table 6 FAB mass spectral data for the $[R_2Sn(S_2COR')_2]$ complexes

Fragment	R = Me	R = Et	R = nBu	R = tBu	R = Ph
R' = Et					
$[RSn(S_2COEt)]^+$	—	—	—	298, 11%	—
$[R_2Sn(S_2COEt)]^+$	—	299, 100%	355, 100%	355, 100%	395, 100%
$[RSn(S_2COEt)_2]^+$	—	391, 16%	419, 11%	419, 8%	—
$[R_2Sn(S_2COEt)_2]^+, [M]^+$	392, 100%	420, 3%	476, 2%	476, 3%	—
$[R_2Sn_2S(S_2COEt)]^+$	—	449, 1%	—	—	—
$[RSn_2(S_2COEt)_2]^+$	—	509, 3%	—	—	—
$[Sn_2(S_2COEt)_3]^+$	—	601, 2%	—	—	—
$[Sn_2(S_2COEt)_4]^+$	—	722, 6%	—	—	—
R' = iPr					
$[R_2Sn(S_2COiPr)]^+$	—	313, 100%	369, 100%	369, 100%	409, 100%
$[RSn(S_2CO)_2]^+$	—	333, 5%	—	—	381, 7%
$[R_2Sn(S_2COiPr)(S_2C)]^+$	361, 61%	—	—	—	—
$[RSn(S_2COiPr)(S_2CO)]^+$	—	376, 4%	—	—	424, 5%
$[RSn(S_2COiPr)_2]^+$	405, 67%	419, 20%	447, 8%	447, 27%	467, 5%
$[R_2Sn(S_2COiPr)_2]^+, [M]^+$	420, 44%	448, 1%	504, 2%	—	544, 3%
$[R_2Sn_2(S_2COiPr)(SC)]^+$	465, 44%	—	—	—	—
$[R_4Sn_2(S_2COiPr)_3]^+$	703, 100%	759, 3%	871, 1%	—	—
R' = cHex					
$[R_2Sn(S_2COCcHex)]^+$	—	353, 100%	409, 100%	409, 100%	—
$[R_2Sn(S_2CO)]^+$	—	—	—	—	366, 100%
$[R_2Sn_2(S_2CO)]^+$	—	388, 8%	—	—	—
$[RSn(S_2COCcHex)(S_2CO)]^+$	402, 100%	—	—	—	—
$[R_3Sn_2(S_2CO)]^+$	—	417, 10%	472, 7%	—	—
$[RSn(S_2COCcHex)_2]^+$	—	499, 9%	527, 13%	527, 6%	547, 45%
$[R_2Sn(S_2COCcHex)_2]^+, [M]^+$	500, 8%	528, 2%	584, 4%	—	624, 39%
$[R_4Sn_2(S_2COCcHex)_3]^+$	—	879, 7%	—	—	—

recently.²⁰ The disparity between the two angles may be related to solid-state effects underlying the difficulty in such correlations.

The availability of two crystal structures of the general formula $[Ph_2Sn(S_2COR')_2]$, i.e. in which the nature of the xanthate-bound R' group has been varied, enables a comparison of the relative coordinating ability of the two xanthate ligands. The $\Delta Sn-S$ values (where $\Delta Sn-S$ is the average difference between the short and long Sn-S bonds formed by the xanthate ligands) of 0.651 and 0.632 Å for the R' = Et and R' = iPr¹¹ compounds, respectively, suggest that the isopropyl xanthate ligand is the better chelating ligand. Similarly it is possible to compare the Lewis acidities of the Me₂Sn and Ph₂Sn moieties as there are two compounds with the formula $[R_2Sn(S_2COEt)_2]$ that have been structurally characterized. A $\Delta Sn-S$ value of 0.626 Å is found for the $[Me_2Sn(S_2COEt)_2]$ ¹⁰ compound (cf. 0.651 Å for the R = Ph compound) which may reflect the enhanced Lewis acidity of the Me₂Sn moiety compared to that of the Ph₂Sn moiety or additional

steric pressure in the latter.

It is noteworthy that the R = Me and Ph compounds adopt essentially the same structure in the solid state, which is in contrast to the related dithiocarbamate complexes. The $[Me_2Sn(S_2CNET_2)_2]$ compounds (there are three polymorphs and four independent molecules) adopt structures related to that shown in Fig. 1^{21,22} whereas the $[Ph_2Sn(S_2CNET_2)_2]$ compound features an approximately *cis* configuration of the phenyl groups and reduced asymmetry in the mode of coordination of the dithiocarbamate ligands.²³

Owing to instability in the X-ray beam, full crystallographic characterization could not be obtained for the $[tBu_2Sn(S_2COR')_2]$, R = Et and iPr, compounds. However, unit-cell data obtained suggest that these compounds have similar structures to that reported for $[Ph_2Sn(S_2COEt)_2]$:

Unit cell data for $[tBu_2Sn(S_2COEt)_2]$: monoclinic, space group $P2_1/n$, $a = 9.572(2)$, $b = 14.401(4)$,

Table 7 Selected bond distances (Å) and angles (deg.) for [Ph₂Sn(S₂COEt')₂]

Atoms	Distance	Atoms	Distance
Sn-S(1)	2.486(1)	Sn-S(3)	2.484(1)
Sn-S(2)	3.052(1)	Sn-S(4)	3.220(1)
Sn-C(11)	2.123(3)	Sn-C(21)	2.123(3)
S(1)-C(1)	1.732(4)	S(3)-C(4)	1.742(4)
S(2)-C(1)	1.641(4)	S(4)-C(4)	1.633(4)
C(1)-O(1)	1.322(5)	C(4)-O(2)	1.319(4)
O(1)-C(2)	1.472(6)	O(2)-C(5)	1.459(5)
Atoms	Angle	Atoms	Angle
S(1)-Sn-S(2)	64.1(1)	S(1)-Sn-S(3)	83.9(1)
S(1)-Sn-S(4)	145.0(1)	S(1)-Sn-C(11)	109.5(1)
S(1)-Sn-C(21)	114.1(1)	S(2)-Sn-S(3)	147.7(1)
S(2)-Sn-S(4)	150.7(1)	S(2)-Sn-C(11)	88.1(1)
S(2)-Sn-C(21)	84.3(1)	S(3)-Sn-S(4)	61.6(1)
S(3)-Sn-C(11)	107.8(1)	S(3)-Sn-C(21)	106.2(1)
S(4)-Sn-C(11)	78.4(1)	S(4)-Sn-C(21)	83.1(1)
C(11)-Sn-C(21)	126.5(1)	Sn-S(1)-C(1)	94.4(1)
Sn-S(2)-C(1)	77.5(1)	Sn-S(3)-C(4)	98.1(1)
Sn-S(4)-C(4)	75.6(1)	S(1)-C(1)-S(2)	124.0(2)
S(1)-C(1)-O(1)	109.5(3)	S(2)-C(1)-O(1)	126.4(3)
S(3)-C(4)-S(4)	124.7(2)	S(3)-C(4)-O(2)	109.8(3)
S(4)-C(4)-O(2)	125.6(3)	C(1)-O(1)-C(2)	119.1(4)
C(4)-O(2)-C(5)	119.5(3)		

$c = 16.305(11)$ Å and $\beta = 107.05(3)^\circ$.

[tBu₂Sn(S₂COiPr)₂]: monoclinic, space group $P2_1/n$, $a = 12.928(4)$, $b = 12.696(11)$, $c = 15.247(11)$ Å and $\beta = 106.41(4)^\circ$.

Table 8 Biological activity for selected [R₂Sn(S₂COR')₂] compounds

R	R'	ID ₅₀ (μmol dm ⁻³) ²	n
Me	Et	>20	3
Me	iPr	>25	2
Me	cHex	>20	3
Et	Et	3.67 ± 0.84	5
Et	cHex	4.12 ± 0.48	5
nBu	cHex	0.16 ± 0.01	4
Ph	Et	1.08 ± 0.26	4
Ph	iPr	0.55 ± 0.18	4
Ph	cHex	1.03 ± 0.49	5
Cisplatin		0.6	
Carboplatin		12	

^a Dose of compound causing 50% growth inhibition of L1210 mouse leukaemia cells in culture after 48 h exposure to the compound. Results are expressed as mean ± standard deviation.

Several of the [R₂Sn(S₂COR')₂] compounds were screened *in vitro* for their anti-tumour activity against L1210 mouse leukaemia cells. An examination of the results summarized in Table 8 suggests the following conclusions:

- (1) diorganotin bisxanthates in general show some activity,
- (2) the Me₂Sn derivatives show little activity; and
- (3) the most active compounds are those with nBu₂Sn or Ph₂Sn moieties.

Although it is difficult to compare the results of *in vitro* tests performed in different laboratories, it is clear that the thiolate compounds reported herein show promising activity, at this early stage, comparable with that found in organotin derivatives containing oxygen and/or nitrogen ligands.^{5,6} Further studies, including testing in animal models, are under way to investigate further the antitumor activity and toxicity of this particular class of compound.

Acknowledgements The Australian Research Council is thanked for support of the crystallographic facility. Technical assistance with the biological testing by Ms V Nink is gratefully acknowledged.

REFERENCES

1. Davies, A G and Smith, P J In: *Comprehensive Organometallic Chemistry*, vol. 2, Wilkinson, G, Stone, F G A and Abel, E W (eds), Pergamon Press, Oxford, 1982, chapter 11
2. Evans, C J and Karpel S *Organotin Compounds in Modern Technology*, J. Organomet. Chem. Library, vol. 16, Elsevier, Amsterdam, 1985
3. Blunden, S J, Cussack, P A and Hill, R *The Industrial Use of Tin Chemicals*, Royal Society of Chemistry, London, 1985
4. Omae, I *Organotin Chemistry*, J. Organomet. Chem. Library, vol. 21, Elsevier, Amsterdam, 1989
5. Gielen, M Tin as a vital nutrient: implications in cancer prophylaxis and other physiological processes. In: *Antitumour Active Organotin Compounds*, Cardarelli, N F (ed.), CRC Press, 1986, Chapter 13
6. Haiduc, I and Silvestru, C *Coord. Chem. Rev.*, 1990, 99: 253
7. Haiduc, I, Silvestru, C and Gielen, M *Bull. Soc. Chim. Belg.*, 1984, 92: 187
8. Huber, F, Roge, G, Carl, L, Atassi, G, Spreafico, F,

- Filippeschi, S, Barbieri, R, Silvestri, A, Rivarola, E, Ruisi, G, DiBianca, F and Alonzo, G *J. Chem. Soc., Dalton Trans.*, 1985, 523
9. Barbieri, R, Silvestri, A, Filippeschi, S, Magistrelli, M and Huber, F *Inorg. Chim. Acta*, 1990, 177: 141
10. Dakternieks, D, Hoskins, B F, Tiekink, E R T and Winter, G *Inorg. Chim. Acta*, 1984, 85: 215
11. Donoghue, N and Tiekink, E R T *J. Organomet. Chem.*, 1991, 420: 179
12. Dakternieks, D, Hoskins, B F, Jackson, P A, Tiekink, E R T and Winter, G *Inorg. Chim. Acta*, 1985, 101: 203
13. Tiekink, E R T and Winter, G *J. Organomet. Chem.*, 1986, 314: 85
14. Edwards, A J, Hoskins, B F and Winter, G *Acta Crystallogr. C*, 1988, 44: 1541
15. Mirabelli, C K, Hill, D T, Faucette, L F, McCabe, L F, Girard, G R, Bryan, D B, Sutton, B M, Bartus, J O, Crooke, S T and Johnson, R K *J. Med. Chem.*, 1987, 30: 2181
16. Siasios, G, Tiekink, E R T and Whitehouse, M W (unpublished results)
17. Sheldrick, G M SHELX76, Program for crystal structure determination, Cambridge University, UK, 1976
18. Johnson, C K ORTEP-II Report ORNL-5138, Oak Ridge National Laboratory, Tennessee, USA, 1976
19. Winter, G *Rev. Inorg. Chem.*, 1980, 2: 253
20. Holecek, J, Handlir, K, Nadvornik, M and Lyck., A *Z. Chem.*, 1990, 30: 265
21. Morris, J S and Schlemper, E O *J. Cryst. Molec. Struct.*, 1979, 9: 13
22. Lockhart, T P, Manders, W F, Schlemper, E O and Zuckermann, J J *J. Am. Chem. Soc.*, 1986, 108: 4074
23. Lindley, P F and Carr, P *J. Cryst. Molec. Struct.*, 1974, 4: 173